Synthesis and characterization of cationic dinuclear complexes of platinum with bridging hydrides; crystal structures of $[Pt_2(\mu\text{-}H)_2\{Bu^t_2P(CH_2)_3PBu^t_2\}_2][BF_4]_2$ and $[Pt_2(\mu\text{-}H)_2\{(C_6H_{11})_2P(CH_2)_3P(C_6H_{11})_2\}_2][BF_4]_2$

Laura Mole,*[a] John L. Spencer,[a] Stephen A. Litster,[a] Alan D. Redhouse,[a] Nicholas Carr[b] and A. Guy Orpen[b]

[a] *Chemical Sciences Division, Science Research Institute, University of Salford, Salford M5 4WT, UK*
[b] *School of Chemistry, University of Bristol, Bristol BS8 1TS, UK*

A series of diplatinum dications $[Pt_2(\mu\text{-}H)_2(L\text{–}L)_2][BF_4]_2$ [L–L = $(C_6H_{11})_2P(CH_2)_nP(C_6H_{11})_2$, $Bu^t_2P(CH_2)_nPBu^t_2$, n = 2 or 3] with two chelating diphosphine and two bridging hydride ligands has been prepared by the elimination of ethene from the agostic alkyl complexes $[PtEt(L\text{–}L)]^+$ or alkene–hydride complexes $[PtH(C_2H_4)(L\text{–}L)]^+$, or by the reaction of the dihydride complexes $[PtH_2(L\text{–}L)]$ with an excess of $HBF_4\cdot OMe_2$. The complexes have been characterized by multinuclear (^1H, ^{31}P and ^{195}Pt) NMR spectroscopy and for $[Pt_2(\mu\text{-}H)_2\{Bu^t_2P(CH_2)_3PBu^t_2\}_2][BF_4]_2$ and $[Pt_2(\mu\text{-}H)_2\{(C_6H_{11})_2P(CH_2)_3P(C_6H_{11})_2\}_2][BF_4]_2$ by single-crystal X-ray crystallography. The latter complex has a structure in which the platinum and phosphorus atoms are coplanar whereas in the former the co-ordination planes of the platinum atoms are twisted with respect to each other by 36.6°. The twisting in $[Pt_2(\mu\text{-}H)_2\{Bu^t_2P(CH_2)_3PBu^t_2\}_2][BF_4]_2$ is ascribed to the steric pressure of the large diphosphine which destabilises the planar geometry. Significantly this complex is fluxional on the NMR time-scale at 290 K whereas the others are static and there is a shift in colour from yellow to red for the strained complex. The dinuclear species are useful synthetic precursors of the $[PtH(L\text{–}L)]^+$ fragment, particularly when L–L is large. Thus $[Pt_2(\mu\text{-}H)_2\{Bu^t_2P(CH_2)_3PBu^t_2\}_2]^{2+}$, which has the most sterically demanding diphosphine, reacts with alkenes [*e.g.* ethene (reversibly) or norbornene] to form mononuclear alkyl complexes with a three-centre, two-electron (agostic) bond.

There is a surprising diversity of diplatinum complexes with two or more hydride ligands, and these have attracted interest because of the range of structures and the unusual spectroscopic properties they display. Early examples were the neutral 28-electron complexes $[\{Pt(\mu\text{-}H)(SiR_3)(PR'_3)\}_2]^1$ (R = alkyl, aryl, alkoxy or Cl; R′ = C_6H_{11}) **1** which were shown to be easily cleaved by electron-pair donors and which also function as excellent hydrosilylation catalysts. A number of monocationic species have also been observed including several 30-electron complexes of general formula $[Pt_2H_3L_4]^+$ (L = monodentate tertiary phosphine or L_2 = diphosphine). Venanzi and co-workers[2] reported the monodentate phosphine complex **2** with distinct platinum centres and non-fluxional hydride ligands, whereas **3**, formed with a chelating diphosphine, has a different structure within which the hydrides exchange freely on the NMR time-scale.[3,4] In both cases the co-ordination environments of the platinum centres are different. An alternative structural type **4** with identical platinum centres and fluxional hydride ligands was observed[5] with the very bulky chelating diphosphine $Bu^t_2P(CH_2)_3PBu^t_2$. The structure and properties of the ancillary ligands are clearly an important factor in determining the characteristics of the diplatinum species. A good example is provided by the diphosphine $Ph_2PCH_2PPh_2$ which has phosphorus lone pairs well oriented for bridging and which consequently affords[4,6] a dinuclear complex with an A-frame structure **5** in which the hydrides do not rapidly exchange. Rarely, isomers have been reported, for example Paonessa and Trogler[7] have noted that $[Pt_2H_3(PEt_3)_4]^+$ may exist in two forms, one **6a** analogous to **2** and a less-stable isomer **6b** with a *trans* co-ordination geometry at both platinum centres.

Neutral complexes are not as numerously reported as the cationic species, although Nixon and co-workers[8] have synthesised the 30-electron dihydride $[Pt_2H_2(dppe)_2]$ [dppe = 1,2-bis(diphenylphosphino)ethane] **7a** and shown that it is a strong base and forms the conjugate acid **3** in the presence of protic solvents such as methanol. Very recently Schwartz and Anderson[9] have published a detailed study of several neutral diplatinum dihydrides of type **7** and shown that they have a structure with terminal hydride bonding both in solution and in the crystalline state {**7b** [L_2 = $Pr^i_2P(CH_2)_2PPr^i_2$, dippe)]}. The two halves of the molecule are held together by an unsupported single Pt–Pt bond. In solution the hydride ligands exchange rapidly on the NMR time-scale at room temperature.

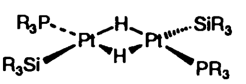
1

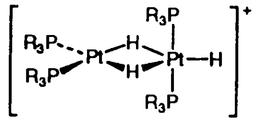
2 R = Ph
6a R = Et

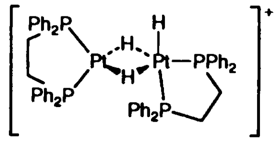
3

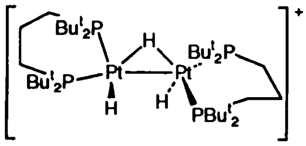
4

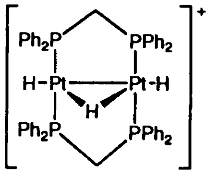
5

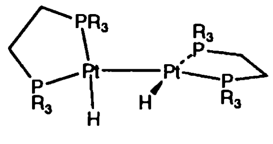
7a R = Ph
7b R = Bu^t

Although palladium and nickel hydride complexes are generally less stable than their platinum counterparts, there are some examples of dinuclear palladium and nickel complexes, for example $[Pd_2(\mu\text{-}H)_2(dippp)_2]$ and the unusual 30-electron lithio-bridged species $[Pd_2(\mu\text{-}H)_2(\mu\text{-}LiBEt_4)(dippp)]$ [dippp = 1,3-bis(diisopropylphosphino)propane] reported by Fryzuk *et al.*[10] and the nickel complex $[Ni_2(\mu\text{-}H)_2(dcpp)_2]$ [dcpp = 1,3-bis(dicyclohexylphosphino)propane].[11]

The adjoining groups also provide interesting examples of dimetallic hydrido complexes. In Group 9, for example, a number of 28-electron complexes of the type $[Rh_2(\mu\text{-}H)_2(PR_3)_4]$[12] ($PR_3$ = triisopropyl phosphite or $\frac{1}{2}$dippe) have been reported. Interestingly several of these complexes readily add dihydrogen to afford $[Rh_2H_4(PR_3)_4]$ with one rhodium having quasi-octahedral geometry[13] whereas the other is in a square-planar or five-co-ordinate environment. Group 11 provides the example of the 32-electron copper complex[14] $[Cu_2(\mu\text{-}H)_2\{(PPh_2CH_2)_3CMe\}_2]$ in which the potentially tridentate phosphine adopts a bidentate structure.

Our research into the extent of steric control by bulky chelating diphosphines of the ground state of mononuclear platinum alkyl compounds has been the subject of recent papers.[15] During the course of this work we noted the formation of diplatinum complexes as the decomposition products of the mononuclear alkyls. We report here the synthesis, structure and spectroscopic properties of a new series of bridging dihydridodiplatinum cations $[Pt_2(\mu\text{-}H)_2(L\text{–}L)_2]^{2+}$ the nature of which is controlled by the size of the diphosphine (L–L). The application of these compounds in synthesis as a source of the $[PtH(L\text{–}L)]^+$ fragment is also described.

Results and Discussion

During our studies of a series of platinum alkyl complexes stabilised by β-agostic interactions[15] we discovered the 28-electron dinuclear complexes $[Pt_2(\mu\text{-}H)_2(L\text{–}L)_2][BF_4]_2$ [L–L = $(C_6H_{11})_2P(CH_2)_2P(C_6H_{11})_2$ (dcpe) **8**, $Bu^t_2P(CH_2)_2PBu^t_2$ (dbpe) **9**, $(C_6H_{11})_2P(CH_2)_3P(C_6H_{11})_2$ (dcpp) **10** and $Bu^t_2P(CH_2)_3PBu^t_2$ (dbpp) **11**] which resulted from the loss of ethene by β elimination from the complexes $[PtEt(L\text{–}L)]^+$ (Scheme 1). The dinuclear complexes **8**–**11**, isolated from dichloromethane–diethyl ether solutions of the mononuclear ethylplatinum complexes as yellow crystals in the case of **8**–**10** and red crystals in the case of **11**, have been characterised by multinuclear (^1H, ^{31}P and ^{195}Pt) NMR and IR spectroscopy (Table 1 and Experimental section). Significantly, the ethyl cation with a larger chelating diphosphine, $o\text{-}C_6H_4(CH_2PBu^t_2)_2$ proved to be stable to decomposition by this route although it has been shown to exchange ethene very readily.

The complexes **9** and **11** have also been prepared separately by protonation with an excess of $HBF_4\cdot OEt_2$ of the corresponding mononuclear diphosphine dihydride complexes $[PtH_2(L\text{–}L)]$ in solution in toluene. Again, attempts to make a dihydride dication with the bulky $o\text{-}C_6H_4(CH_2PBu^t_2)_2$ ligand by this method were not successful although there was evidence for the formation of the corresponding trihydride cation analogous to **4**.

In the ^1H NMR spectrum of complex **11** recorded at 298 K the hydride resonance is observed as a binomial quintet [$^2J(PH)$ = 31 Hz] centred on δ 0.22 with platinum satellites in a 1:8:18:8:1 ratio and $^1J(PtH)$ 767 Hz, indicating the equivalence of the hydrides with coupling to four equivalent phosphorus and two equivalent platinum nuclei. The spectrum is consistent with a molecule in which there is rotation of the two co-ordination planes about the metal–metal axis.

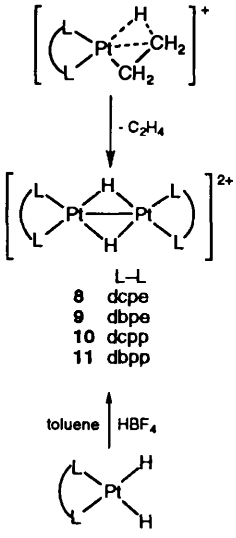

Scheme 1

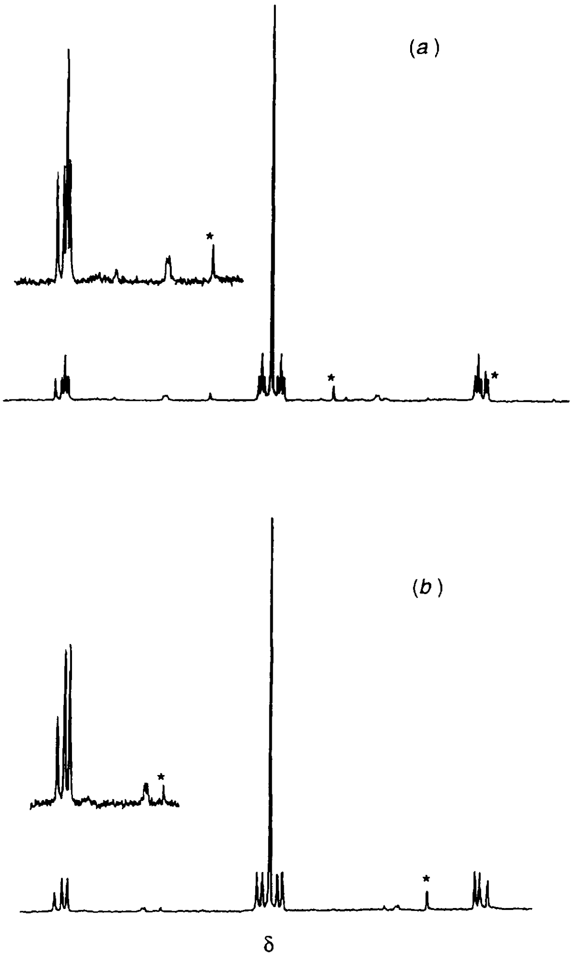

Fig. 1 The ^{31}P NMR spectra, measured at room temperature, of complexes **11** (*a*) and **9** (*b*). Asterisks denote impurities

Variable-temperature NMR spectroscopic studies confirm that cation **11** is fluxional in solution. The ^1H NMR spectrum recorded at 195 K shows the hydride signal as a triplet with ^{195}Pt satellites [$^2J(PH)$ 62 and $^1J(PtH)$ 790 Hz] consistent with the limiting spectrum of a planar or quasi-planar dinuclear $[P_2Pt(\mu\text{-}H)_2PtP_2]$ core in which $^2J(PH)$ 62 Hz represents a *trans* coupling to two of the phosphorus nuclei whereas the *cis* coupling is too small to be observed under these conditions. Similarly, the $^{31}P\text{-}\{^1H\}$ NMR spectrum recorded at 193 K shows the central resonance at δ 61 with the platinum satellites appearing as doublets [$^3J(PP)$ 40 Hz] consistent with only *trans* phosphorus–phosphorus coupling being observed. In contrast, at 298 K the satellites appear as triplets [$^3J(PP)$ 20 Hz] [Fig. 1(*a*)] which suggests rapid rotation about the metal–metal axis

Table 1 Infrared ($\tilde{\nu}_{max}$/cm^{-1}) and selected ^{31}P NMR[a] spectroscopic data for the complexes $[Pt_2(\mu\text{-}H)_2(L\text{-}L)_2]^{2+}$ **8**–**11**

	Compound	Colour	IR	^{31}P NMR δ	 ^1J(PtP)/Hz	 ^2J(PtP)/Hz	 ^3J(PP)/Hz
8	$[Pt_2(\mu\text{-}H)_2(dcpe)_2][BF_4]_2$	Yellow	1644	96	2758	134	26
9	$[Pt_2(\mu\text{-}H)_2(dbpe)_2][BF_4]_2$	Yellow	1631	119[b]	2880	139	35
10	$[Pt_2(\mu\text{-}H)_2(dcpp)_2][BF_4]_2$	Yellow	1634	39	2721	138	29
11	$[Pt_2(\mu\text{-}H)_2(dbpp)_2][BF_4]_2$	Red	1629	61[c]	2861	133	20[d]

[a] Measured in CH_2Cl_2 at ambient temperature. [b] J(PtPt) 1280 Hz. [c] J(PtPt) 1820 Hz. [d] Average value, see text.

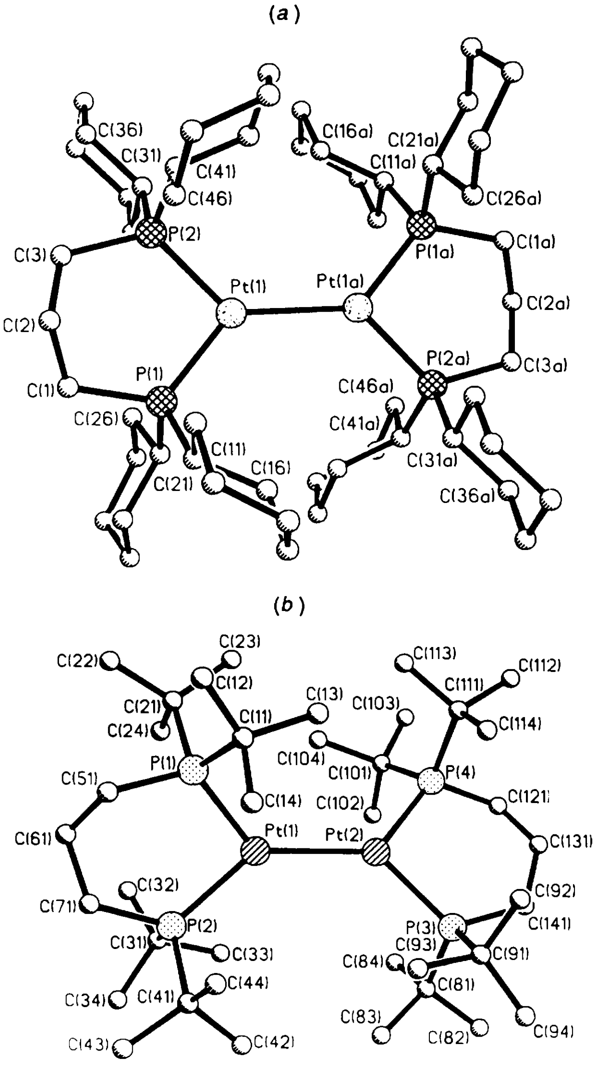

Fig. 2 Molecular structure of the dications **10** (*a*) and **11** (*b*) showing the heavy-atom positions and the atom labelling scheme

(see below). The spectrum also reveals lines arising from the isotopomer with two ^{195}Pt nuclei, from which J(Pt–Pt) was calculated to be 1820 Hz.

The ^{31}P NMR data for compounds **8**–**10** recorded at ambient temperature are summarised in Table 1. In contrast to **11**, the data are consistent with a planar structure in which rotation about the Pt–Pt bond is slow on the NMR time-scale. A planar structure in solution is in accordance with the planar solid-state structure established for **10** as discussed below. For example the spectrum of **9** recorded at ambient temperature [Fig. 1(*b*)] shows the central resonance at δ 119 with platinum satellites as doublets similar to the spectrum of **11** recorded at 193 K. Examination of the ^{1}H NMR spectrum of **9** reveals that the central signal for the bridging hydrides is obscured by that of the phosphine *tert*-butyl groups but the satellites of the hydride signal are clearly visible separated by J(PtH) of 786 Hz. Further corroboration of the presence of two bridging hydrides is obtained from the proton-coupled ^{195}Pt NMR spectra of complexes **8** and **9**. In each case the spectrum recorded at ambient temperature shows coupling to two hydride ligands with ^1J(PtH) of 796 and 786 Hz respectively. For all four compounds, broad bands are observed in the IR spectra at 1629–1644 cm^{-1} (see Table 1) in the bridging metal hydride region and are assigned to ν(Pt–H–Pt).

The structures of complexes **10** and **11** in the solid state (as BF_4^- salts with dichloromethane of crystallisation) (Fig. 2) were determined at 233 and 203 K respectively by single-crystal X-ray crystallographic studies. The crystallographic data are summarised in Table 2, bond lengths and selected bond angles are collected in Tables 3 and 4 respectively. The cation in **10** has a crystallographically imposed centre of symmetry which requires the P_4Pt_2 unit to be exactly planar. The approximate symmetry of the core is D_{2h}. However, when the position of the cyclohexyl groups is taken into consideration the symmetry of the dication as a whole is nearly C_{2h}. In contrast, in the cation **11**, where there is no imposed symmetry, the P_4Pt_2 unit is not planar and the core has approximate D_2 symmetry. Distortion of four-co-ordinate d^8 complexes from square-planar geometry is not unknown and the distortion in **11** is similar to that seen in $[PtEt_2(dbpp)]$.[15c] The analysis failed to locate the bridging hydrides in either complex although the spectroscopic evidence strongly suggests that they are coplanar with the P_4Pt_2 unit in **10** and symmetrically bridge the Pt–Pt bond. In the case of **11** the hydrides presumably lie on an axis which bisects the dihedral angle between the P_2Pt planes.

The dynamic behaviour of complex **11** may now be discussed in the light of the structural results. Scheme 2 shows the cation viewed down the Pt–Pt axis with the PtP_2 planes represented as lines, and **A** and **A′** correspond to the structure in the crystal which is consistent with the NMR spectra at low temperature. The spectrum at room temperature may be explained by assuming a rotation about the Pt–Pt axis which involves both **B** and **B′**. Conversion of **A** into **A′** *via* a planar geometry (central equilibrium) does not lead to exchange of any of the nuclei, and the NMR experiments provide no evidence of whether this process occurs on the NMR time-scale. The factor differentiating **11** from **8**–**10** is the bulk of the diphosphine which destabilises the in-plane geometry (or quasi-in-plane **A**) relative to the perpendicular geometry **B** and thus lowers the activation energy to rotation about the Pt–Pt axis.

Table 5 compares selected structural parameters for **10** and **11** with those of related mono- and di-nuclear species containing the Pt(dbpp) fragment. The data suggest that cation **11** is significantly more strained than **10**. Both the Pt–Pt bond length and the average Pt–P bond distances in **11** are significantly longer than the corresponding distances in **10**. Nevertheless, the Pt–Pt and Pt–P distances in **11** are comparable with the corresponding bond distances in the related complexes[5,16] **4** and $[Pt_2(dbpp)_2]$ **12**. Interestingly, **11** is significantly more active than **10** in reactions which involve cleavage of the Pt–Pt bond. This enhanced reactivity is presumably a result of the strain placed on the metal–metal

Table 2 Crystallographic data for $[Pt_2(\mu\text{-}H)_2\{(C_6H_{11})_2P(CH_2)_3P(C_6H_{11})_2\}_2][BF_4]_2\cdot 2CH_2Cl_2$ **10** and $[Pt_2(\mu\text{-}H)_2\{Bu^t{}_2P(CH_2)_3PBu^t{}_2\}_2][BF_4]_2\cdot 2CH_2Cl_2$ **11**

	10	**11**
Empirical formula	$C_{54}H_{104}B_2F_8P_4Pt_2\cdot 2CH_2Cl_2$	$C_{38}H_{86}B_2F_8P_4Pt_2\cdot 2CH_2Cl_2$
M	1582.9	1398.6
Space group	$P\bar{1}$	$P2_1/n$
Crystal symmetry	Triclinic	Monoclinic
Crystal size/mm	0.20 × 0.14 × 0.10	0.35 × 0.20 × 0.20
a/Å	12.147(2)	21.505(8)
b/Å	12.825(3)	11.474(3)
c/Å	12.842(3)	22.857(6)
α/°	113.87(2)	
β/°	102.97(2)	100.62(3)
γ/°	106.92(2)	
Z	1	4
U/Å^3	1624.6	5544(3)
D_c/Mg m^{-3}	1.618	1.676
μ(Mo-Kα)/mm^{-1}	4.664	5.456
2θ range/°	3–50	3–50
$F(000)$	794	2776
Reflections collected	6030	10 660
Unique reflections (R_{int})	5736 (0.0774)	9761 (0.0430)
Observed reflections	4579 [$F > 4.0\sigma(F)$]	4684 [$F > 6\sigma(F)$]
g in weighting scheme [$w^{-1} = \sigma^2(F) + gF^2$]	0.0004	0.001
No. variables	343	511
R	4.49	6.41
R'	4.66	7.73
S	1.27	1.65
Maximum, minimum in ΔF synthesis/e Å^{-3}	1.89, −0.87	2.34, −2.60

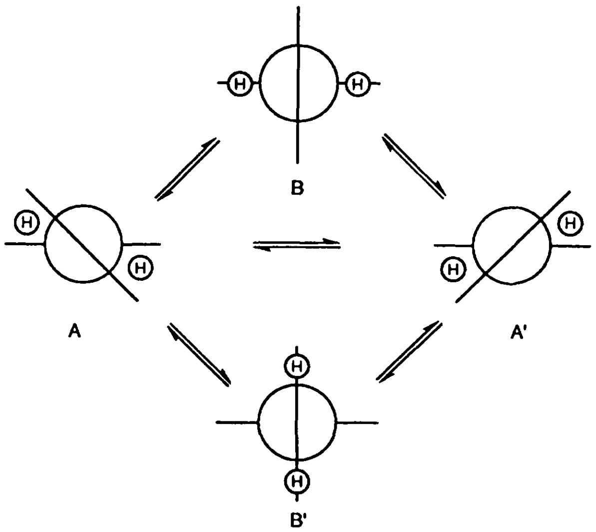

Scheme 2

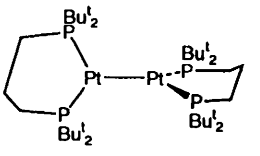

12

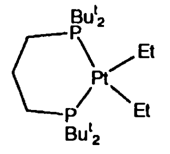

13

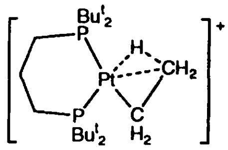

14

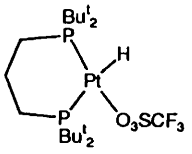

15

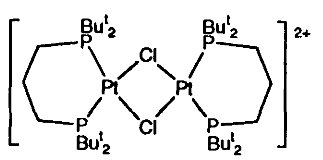

16

bond by the non-bonding interactions between *tert*-butyl groups. The observed twisting of the platinum co-ordination planes in **11** by 36.6° from coplanarity is presumably also a consequence of the strong non-bonded interactions between the *tert*-butyl groups of the two dbpp ligands. The main point is that, in the cations prepared, planarity of the P_4Pt_2 unit appears to be preferred, presumably for electronic reasons. However, increasing bulkiness of the diphosphine substituents leads to non-planarity in the case of **11**. The chelate angles in **10** and **11** are not significantly different but as the dihedral angle between the P_2Pt planes increases we would expect the chelate bite angles to increase because of the improved accommodation of the phosphine substituents. The largest bite angle is in **12** (Table 5) where the P_2Pt planes are perpendicular and there are no restraining hydrides. However, it should be noted that **12** is a platinum(0) species and could be expected to favour a P–Pt–P angle of 120° whereas **10** and **11** are platinum(II) complexes and the bite angle may be constrained for electronic as well as steric reasons. Although the bite angle of a chelating diphosphine is determined in part by the length of the chain linking the two phosphorus atoms, the non-bonded interactions must also restrict the angle to minimise repulsive contacts in the immediate co-ordination sphere of the metal and between the bulky substituents of the diphosphine ligands.

Although complexes **4** and **12** are not strictly comparable with the compounds under discussion the order of increasing Pt–Pt bond lengths are **10** (2.698), **11** (2.726), **12** (2.765), **4** (2.768 Å). This parameter might be expected to be the most sensitive to twisting of the P_2Pt planes. The weakening of the Pt–H–Pt link by this twisting is reflected by the increased reactivity of **11** over **8**–**10** which have smaller diphosphine ligands. It appears that the structure and reactivity of the complexes are directly related to and dependent on the size of the bite angle and the bulk of the substituents on the chelating diphosphine. For **11**, the complex with the largest chelate, the breaking of the Pt–Pt bond is facile (Scheme 3). Complex **11**

Table 3 Bond lengths (Å) for complexes **10** and **11** excluding distances to hydrogen

Compound **10**

Pt(1)–P(1)	2.239(3)	Pt(1)–P(2)	2.239(2)
Pt(1)–Pt(1a)	2.698(1)	P(1)–C(1)	1.818(7)
P(1)–C(11)	1.826(11)	P(1)–C(21)	1.828(11)
P(2)–C(3)	1.800(9)	P(2)–C(31)	1.819(11)
P(2)–C(41)	1.824(12)	C(1)–C(2)	1.50(1)
C(2)–C(3)	1.52(2)	C(11)–C(12)	1.51(2)
C(11)–C(16)	1.51(4)	C(12)–C(13)	1.53(2)
C(13)–C(14)	1.48(1)	C(14)–C(15)	1.52(2)
C(15)–C(16)	1.50(2)	C(21)–C(22)	1.52(2)
C(21)–C(26)	1.54(2)	C(22)–C(23)	1.51(2)
C(23)–C(24)	1.49(2)	C(24)–C(25)	1.51(2)
C(25)–C(26)	1.52(2)	C(31)–C(32)	1.53(2)
C(31)–C(36)	1.53(1)	C(32)–C(33)	1.51(2)
C(33)–C(34)	1.52(1)	C(34)–C(35)	1.51(2)
C(35)–C(36)	1.52(2)	C(41)–C(42)	1.52(1)
C(41)–C(46)	1.53(2)	C(42)–C(43)	1.53(2)
C(43)–C(44)	1.50(2)	C(44)–C(45)	1.52(2)
C(45)–C(46)	1.51(2)	C(4)–Cl(1)	1.68(2)
C(4)–Cl(2)	1.69(2)	B(1)–F(1)	1.31(2)
B(1)–F(2)	1.34(2)	B(1)–F(3)	1.35(2)
B(1)–F(4)	1.34(2)		

Compound **11**

Pt(1)–Pt(2)	2.726(1)	Pt(1)–P(1)	2.297(6)
Pt(1)–P(2)	2.318(6)	Pt(2)–P(3)	2.318(6)
Pt(2)–P(4)	2.318(6)	P(1)–C(11)	1.90(3)
P(1)–C(21)	1.93(2)	P(1)–C(51)	1.83(2)
P(2)–C(31)	1.86(2)	P(2)–C(41)	1.88(2)
P(2)–C(71)	1.82(2)	P(3)–C(81)	1.87(3)
P(3)–C(91)	1.92(2)	P(3)–C(141)	1.88(2)
P(4)–C(101)	1.85(2)	P(4)–C(111)	1.88(2)
P(4)–C(121)	1.78(2)	C(11)–C(12)	1.52(4)
C(11)–C(13)	1.54(3)	C(11)–C(14)	1.53(4)
C(21)–C(22)	1.56(3)	C(21)–C(23)	1.51(3)
C(21)–C(24)	1.51(4)	C(31)–C(32)	1.44(3)
C(31)–C(33)	1.62(3)	C(31)–C(34)	1.57(3)
C(41)–C(42)	1.56(3)	C(41)–C(43)	1.54(3)
C(41)–C(44)	1.50(3)	C(81)–C(82)	1.56(3)
C(81)–C(83)	1.57(3)	C(81)–C(84)	1.49(3)
C(91)–C(92)	1.51(3)	C(91)–C(93)	1.54(3)
C(91)–C(94)	1.53(3)	C(101)–C(102)	1.50(3)
C(101)–C(103)	1.59(3)	C(101)–C(104)	1.59(3)
C(111)–C(112)	1.54(3)	C(111)–C(113)	1.55(3)
C(111)–C(114)	1.54(3)	C(51)–C(61)	1.53(3)
C(61)–C(71)	1.50(4)	C(121)–C(131)	1.40(4)
C(141)–C(131)	1.42(4)	B(1)–F(11)	1.35(3)
B(1)–F(12)	1.37(4)	B(1)–F(13)	1.34(3)
B(1)–F(14)	1.39(4)	B(2)–F(21)	1.30(4)
B(2)–F(22)	1.33(4)	B(2)–F(23)	1.26(4)
B(2)–F(24)	1.29(5)	Cl(1)–C(15)	1.71(3)
Cl(2)–C(15)	1.67(4)	C(16)–Cl(3)	1.76(5)
C(16)–Cl(4)	1.61(6)		

Table 4 Selected interbond angles (°) for compounds **10** and **11**

Compound **10**

P(1)–Pt(1)–P(2)	95.0(1)	P(1)–Pt(1)–Pt(1a)	132.4(1)
P(2)–Pt(1)–Pt(1a)	132.5(1)	Pt(1)–P(1)–C(1)	120.4(3)
Pt(1)–P(1)–C(11)	113.1(3)	C(1)–P(1)–C(11)	104.3(5)
Pt(1)–P(1)–C(21)	108.4(3)	C(1)–P(1)–C(21)	104.6(5)
C(11)–P(1)–C(21)	104.9(4)	Pt(1)–P(2)–C(3)	120.0(3)
Pt(1)–P(2)–C(31)	109.1(2)	C(3)–P(2)–C(31)	103.8(4)
Pt(1)–P(2)–C(41)	105.7(5)	C(3)–P(2)–C(41)	103.8(5)
		C(31)–P(2)–C(41)	105.7(5)

Compound **11**

Pt(2)–Pt(1)–P(1)	131.4(2)	Pt(2)–Pt(1)–P(2)	134.1(2)
P(1)–Pt(1)–P(2)	94.5(2)	Pt(1)–Pt(2)–P(3)	132.6(1)
Pt(1)–Pt(2)–P(4)	132.8(1)	P(3)–Pt(2)–P(4)	94.6(2)
Pt(1)–P(1)–C(11)	106.5(8)	Pt(1)–P(1)–C(21)	114.5(7)
Pt(1)–P(1)–C(51)	117.3(7)	Pt(1)–P(2)–C(31)	105.4(7)
Pt(1)–P(2)–C(41)	114.8(7)	Pt(1)–P(2)–C(71)	118.4(8)
Pt(2)–P(3)–C(81)	114.1(8)	Pt(2)–P(3)–C(91)	105.0(7)
Pt(2)–P(3)–C(141)	118.3(7)	Pt(2)–P(4)–C(101)	104.8(7)
Pt(2)–P(4)–C(111)	114.3(7)	Pt(2)–P(4)–C(121)	116.9(7)
C(11)–P(1)–C(21)	112.8(11)	C(11)–P(1)–C(51)	101.8(10)
C(21)–P(1)–C(51)	103.4(9)	C(31)–P(2)–C(41)	114.3(11)
C(31)–P(2)–C(71)	105.1(11)	C(41)–P(2)–C(71)	98.9(10)
C(81)–P(3)–C(91)	114.1(10)	C(81)–P(3)–C(141)	100.4(10)
C(91)–P(3)–C(141)	105.0(10)	C(101)–P(4)–C(111)	113.4(11)
C(101)–P(4)–C(121)	104.0(9)	C(111)–P(4)–C(121)	103.2(10)

reacts readily in solution with alkenes to generate mononuclear alkyl agostic complexes with ethene, norbornene (bicyclo[2.2.1]-hept-2-ene) and other alkenes, possibly *via* an unsaturated $[P_2PtH]^+$ fragment (Scheme 3). In contrast, reactions of the complexes **8**–**10** with alkenes are slow; none reacts with C_2H_4 at 1 atm (*ca.* 10^5 Pa) and room temperature, although **9** reacts slowly with norbornene to form the known [15] agostic norbornyl complex with some decomposition.

Complexes **10** and **11** are 28e species, isoelectronic with the $H_2Rh_2P_4$ species first noted by Muetterties and co-workers.[12,13] They form part of a series of $[M_2(\mu\text{-}H)_2L_4]^{n+}$ species (M = Rh, *n* = 0; M = Pt, *n* = 2; M = Ni, Pd or Pt, *n* = 0; M = Cu, *n* = 0) in which the valence-electron count in the dinuclear species ranges from 28 to 32.

Dedieu and Hoffmann[18] studied the bonding in Pt_2L_4 complexes in which the PtL_2 fragments were coplanar (D_{2h} molecular symmetry) or orthogonal (D_{2d}). These complexes are 28e, d^{10} platinum(0) dimers in which there is direct Pt–Pt bonding arising from subtle mixing of s and p hybrid-orbital character into the d^{10}–d^{10} interactions. The Pt $\cdots$ Pt distances in **10** and **11** are very slightly *shorter* than in **12** $[Pt_2(dbpp)_2]$ (2.765 Å) although it is usually accepted that protonation of a metal–metal bond results in *lengthening* as a consequence of a two-centre two-electron M–M bond becoming a three-centre two-electron M–H–M interaction (as seen in **7b** and **4**). In **10** and **11** the formal oxidation state of the Pt atoms is +2 and a strong preference for local square-planar geometry at Pt results. In effect **11** results from formal double protonation of the planar D_{2h} pseudo-symmetry form of **12**. In this formation we can predict the principal effects of adding $2H^+$ symmetrically across the Pt–Pt vector, based on Dedieu and Hoffmann's analysis. The principal interaction will be between the asymmetric combination of the H 1s orbitals and the π_d Pt–Pt orbital (in Dedieu and Hoffmann's nomenclature, Fig. 3). Any interaction between the symmetric combination of H 1s orbitals and platinum orbitals of σ symmetry will be much weaker due to poor spatial overlap of the relevant orbitals. Thus there is likely to be little disruption of the principal Pt–Pt bonding (which is σ in character according to Dedieu and Hoffmann) as a result of the formal double protonation of **12** to give **11**, consistent with the small change in Pt–Pt distance observed.

The interrelationship between the dication **11** described here and the neutral compound **12** and the monocation **4** synthesised by Otsuka and co-workers [5] was a matter of interest to us. In an attempt to establish a synthetic connection between **11** and **12** we treated solutions of **11** with various deprotonating reagents. On reaction with NBu^n_4OH, **11** undergoes homolytic cleavage leading to the formation of a complex assigned the formula [PtH(OH)(dbpp)] on the basis of its ^{31}P NMR spectrum alone [δ 36.5 *J*(PtP) 3347; 21.3, *J*(PtP) 1862; *J*(PP) 15 Hz]. Reaction of **11** with a trace of water results in the formation of $[PtH(OH_2)(dbpp)]^+$ which was detected by ^{31}P and ^1H NMR studies [δ_P 42.5, *J*(PtP) 4221; 30.5, *J*(PtP) 1932, *J*(PP) 9; δ_H −7.5, *J*(PtH) 831, *J*(PH) 173, 16 Hz].

Reaction in dichloromethane solution of complex **11** with H_2 resulted in the formation of $[Pt_2H_3(dbpp)_2]^+$ **4**, which formally represents the oxidative addition of dihydrogen accompanied by deprotonation. This contrasts to the reactivity of the 28e rhodium complexes $[Rh_2(\mu\text{-}H)_2(PR_3)_4]$ which will add H_2 to

Table 5 Comparison of average structural data for complexes **10** and **11** with those for related mono- and di-nuclear complexes

Complex	**10**	**11**	**4**	**7b**	**12**	**13**	**14**	**15**	**16**
Pt–Pt/Å	2.698	2.726	2.768	2.609	2.765				
Mean Pt–P/Å	2.239	2.313	2.304	2.266	2.270	2.324	2.285	2.267	2.294
P–Pt–P/°	95.0	94.5	99.2	89.67	102.6	97.9	100.4	101.3	97.9
Ref.	This work	This work	5	9	16	15(*c*)	15(*c*)	15(*c*)	17

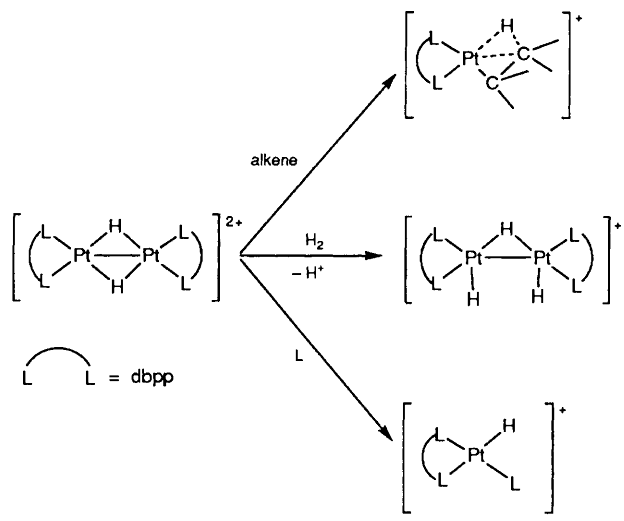

Scheme 3

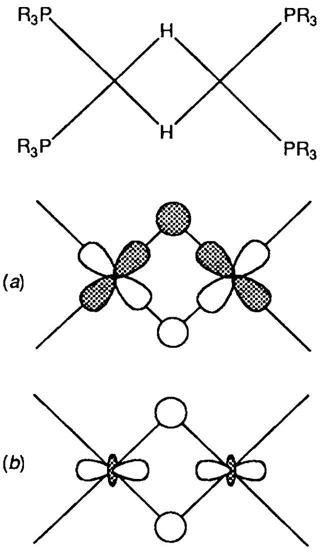

Fig. 3 Orbital interactions in planar diplatinum dications

form dinuclear tetrahydrido complexes. We also considered that it might be possible to convert **11** into an analogue of the neutral dihydrides **7** by reaction with a suitable reducing agent. However, **11** reacted with 2 equivalents of cobaltocene in a complex manner resulting in the formation of $[Pt_2H_3(dbpp)_2]^+$ along with the mononuclear dihydride $[PtH_2(dbpp)]$ as the only products detectable by ^{31}P NMR spectroscopy.

Conclusion

New cationic diplatinum dihydride complexes with chelating tetraalkyldiphosphines are readily synthesised by protonation of the corresponding mononuclear dihydrides. The chemical and spectroscopic properties of the new complexes are dictated by the steric demands of the diphosphine ligand. For the case where the diphosphine is dbpp the diplatinum species is destabilised to the extent that it serves as a useful source of the $[PtH(L\text{–}L)]^+$ fragment in a variety of reactions with electron donors. Complexes **8–11** are readily converted into the corresponding trihydride monocations such as **4** which have been reported previously. However, we were not able to find the reaction conditions which would convert **11** into **12**.

Experimental

All reactions were carried out under a dry, oxygen-free nitrogen atmosphere using standard Schlenk-tube techniques. Solvents were dried thoroughly over appropriate reagents and freshly distilled prior to use. The compounds[16,19] $[PtH_2(dbpp)]$ and $[PtH_2(dbpe)]$ and $[PtH_2\{o\text{-}C_6H_4(CH_2PBu^t_2)_2\}]$ were prepared by treating the corresponding platinum(II) diphosphine dichlorides with an excess of $NaBH_4$ in ethanol. Removal of the solvent *in vacuo* and subsequent extraction with CH_2Cl_2 gave the platinum(II) diphosphine dihydrides in good yield. The compounds $[PtEt(L\text{–}L)]^+$ were prepared by literature methods.[15]

The NMR spectra were recorded on Bruker AC300 or JEOL EX90 pulsed Fourier-transform spectrometers at ambient temperature unless otherwise stated. Proton and carbon-13 chemical shifts are positive to high frequency of $SiMe_4$; phosphorus-31 and platinum-195 chemical shifts positive to high frequency of 85% H_3PO_4 (external) and $\Xi(^{195}Pt)$ 21.4 MHz respectively. Infrared spectra were recorded on a Perkin-Elmer 1710 FTIR spectrophotometer as Nujol mulls between KBr plates.

Synthesis of the complexes

$[Pt_2(\mu\text{-}H)_2(L\text{–}L)_2][BF_4]_2$ [L–L = $(C_6H_{11})_2P(CH_2)_nP(C_6H_{11})_2$ or $Bu^t_2P(CH_2)_nPBu^t_2$ (*n* = 2 or 3)]. *Method* 1. All the dinuclear compounds $[Pt_2(\mu\text{-}H)_2(L\text{–}L)_2][BF_4]_2$ were formed in an identical manner. The compound $[PtEt(L\text{–}L)]^+$ (*ca.* 0.150 g) was dissolved in CH_2Cl_2 (*ca.* 1 cm^3). After standing for a maximum of 24 h at room temperature the solution had changed from colourless to yellow in the cases of **8–10** and to red in the case of **11**. Removal of the solvent *in vacuo* and recrystallisation from CH_2Cl_2–Et_2O afforded clear yellow crystals of **8–10** and clear red ones of **11**. Although a solution of $[PtEt\{o\text{-}C_6H_4(CH_2PBu^t_2)_2\}][BF_4]$ was treated in the same way no reaction to form a dinuclear complex was observed even after a prolonged period.

The complex $[Pt_2(\mu\text{-}H)_2(dcpe)_2][BF_4]_2$ **8** was prepared as yellow microcrystals. NMR (CD_2Cl_2): δ_H 1.0–2.5 (96 H, br, C_6H_{11}, PCH_2); δ_P(proton coupled) 97.3 [t, *J*(PH) 67] (see also Table 1); δ_{Pt} 305 [ttt, *J*(PtP) 2763 and 139, *J*(PtH) 796-Hz]. An analytically pure sample was not obtained. The complex $[Pt_2(\mu\text{-}H)_2(dbpe)_2][BF_4]_2$ **9** was also prepared by method 2. The complex $[Pt_2(\mu\text{-}H)_2(dcpp)_2][BF_4]_2$ **10** was obtained as yellow microcrystals. An analytically pure sample was not obtained. NMR (CD_2Cl_2): δ_H 1.0–2.5 (98 H, br, all dcpp protons).

Method 2. A cold (*ca.* 0 °C) solution of $[PtH_2(dbpe)]$ (0.350 g, 0.68 mmol) in toluene (15 cm^3) was treated with an excess of $HBF_4{\cdot}OMe_2$ (0.5 cm^3) and the resulting mixture allowed to warm to ambient temperature. The supernatant liquid was decanted, and the oily solid washed with OEt_2 (2 × 10 cm^3) and dried *in vacuo* to give **9** as yellow microcrystals (0.695 g, 85%) (Found: C, 36.25; H, 6.90. $C_{36}H_{82}B_2F_8P_4Pt_2$ requires C, 35.95; H, 6.90%). NMR (CD_2Cl_2): δ_H 1.72 (see Discussion) [tt, J(PH) 73 and 7, J(PtH) 786, bridging hydrides], 1.49 [36 H, d, J(PH) 15, CH_3] and 2.2 (6 H, m, PCH_2, PCH_2CH_2); δ_{Pt} 364 [ttt, J(PtP) 2881 and 142, J(PtH) 786 Hz].

The complex $[Pt_2(\mu\text{-}H)_2(dbpp)_2][BF_4]_2$ **11** was obtained as red crystals in 85% yield by either method 1 or 2 (Found: C, 37.15; H, 7.00. $C_{38}H_{86}B_2F_8P_4Pt_2$ requires C, 37.15; H, 7.00%). NMR (CD_2Cl_2): δ_H 0.12 [2 H, qnt, J(PH) 31, J(PtH) 767, $(\mu\text{-}H)_2$], 1.5 [72 H, d, J(PH) 14, CH_3] and 2.2 (6 H, m, PCH_2 and PCH_2CH_2); δ_H (195 K) 0.22 [2 H, t, J(PtH) 790, J(PH) 62, $(\mu\text{-}H)_2$], other peaks remain unchanged; δ_P (193 K) 61.0 [J(PtP) 2843 and 130, J(PP) 40 Hz].

Reactions of complex 11

With H_2. A solution of complex **11** in CD_2Cl_2 was degassed and H_2 bubbled through for 1 hr. A ^1H NMR spectrum showed complete conversion into $[Pt_2H_3(dbpp)_2]^+$ the identity of which[4,5] was confirmed by ^{31}P NMR spectroscopy.

With $NBu^n{}_4OH$. A suspension of complex **11** in toluene was degassed and $NBu^n{}_4OH$ (*ca.* 0.5 cm^3) was added; a change from red to brown was noted. After removal of the toluene *in vacuo* a ^{31}P NMR spectrum in CH_2Cl_2 showed the formation of a mononuclear compound assigned the formula [PtH(OH)(dbpp)]. δ_P 36.5 [J(PtP) 3347] and 21.3 [J(PtP) 1862, J(PP) 15 Hz].

With water. A solution of complex **11** in CH_2Cl_2–tetrahydrofuran was treated with water (*ca.* 0.5 cm^3) and a change from red to yellow was noted. A ^{31}P NMR spectrum showed complete conversion into a mononuclear compound assigned the formula $[PtH(OH_2)(dbpp)]^+$. δ_P 42.5 [J(PtP) 4221] and 30.5 [J(PtP) 1932, J(PP) 9]; δ_H −7.5 [J(PtH) 831, J(PH) 173, 16 Hz].

Crystallography

Structure determination and refinement data for complexes **10** and **11** are given in Table 2. The diffracted intensities were collected on a Siemens R3m/V four-circle diffractometer with Mo-Kα radiation (λ = 0.710 73 Å) using θ–2θ scans at 233 K for **10** and 203 K for **11**. In each case standard reflections were monitored every 100 and the data corrected for the small amount of deterioration recorded. Semiempirical absorption corrections based on ψ scans were applied, maximum, minimum transmission 0.79, 0.97 for **10** and 0.78, 0.90 for **11**. The structures were solved by direct methods and refined using full-matrix least-squares techniques with the SHELXTL PLUS set of programs.[20] Hydrogen atoms were placed in calculated positions and refined riding on the appropriate atom with isotropic thermal parameters. All non-hydrogen atoms were refined on F with anisotropic thermal parameters in **10**. However, the dichloromethane of crystallisation in **11** was disordered: no attempt was made to model the disorder and the carbon and chlorine atoms in this case were refined isotropically.

Atomic coordinates, thermal parameters, and bond lengths and angles have been deposited at the Cambridge Crystallographic Data Centre (CCDC). See Instructions for Authors, *J. Chem. Soc., Dalton Trans.*, 1996, Issue 1. Any request to the CCDC for this material should quote its full literature citation and the reference number 186/21.

Acknowledgements

We acknowledge the financial support of the EPSRC for this work.

References

1 M. Green, J. A. K. Howard, J. Proud, J. L. Spencer, F. G. A. Stone and C. A. Tsipis, *J. Chem. Soc., Chem. Commun.*, 1976, 671.
2 G. Bracher, D. M. Grove, P. S. Pregosin and L. M. Venanzi, *Angew. Chem., Int. Ed. Engl.*, 1979, **18**, 155.
3 G. Minghetti, G. Banditelli and A. L. Bandini, *J. Organomet. Chem.*, 1977, **139**, C80; C. B. Knobler, H. D. Kaesz, G. Minghetti, A. L. Bandini, G. Banditelli and F. Bonati, *Inorg. Chem.*, 1983, **22**, 2324.
4 M. Y. Chaing, R. Bau, G. Minghetti, A. L. Bandini, G. Banditelli and T. F. Koetzle, *Inorg. Chem.*, 1984, **23**, 122.
5 T. H. Tulip, T. Yamagata, T. Yoshida, R. D. Wilson, J. A. Ibers and S. Otsuka, *Inorg. Chem.*, 1979, **18**, 2239.
6 M. P. Brown, R. J. Puddephatt, M. Rashidi and K. R. Seddon, *Inorg. Chim. Acta*, 1977, **23**, L27; M. P. Brown, R. J. Puddephatt, M. Rashidi and K. R. Seddon, *J. Chem. Soc., Dalton Trans.*, 1978, 516.
7 R. S. Paonessa and W. C. Trogler, *Inorg. Chem.*, 1983, **22**, 1083.
8 D. Carmichael, P. B. Hitchcock, J. F. Nixon and A. Pidcock, *J. Chem. Soc., Chem. Commun*, 1988, 1554.
9 D. J. Schwartz and R. A. Anderson, *J. Am. Chem. Soc.*, 1995, **117**, 4014.
10 M. D. Fryzuk, B. R. Lloyd, G. K. B. Clentsmith and S. J. Rettig, *J. Am. Chem. Soc.*, 1991, **113**, 4332; 1994, **116**, 3804.
11 K. Jonas and G. Wilke, *Angew. Chem., Int. Ed. Engl.*, 1970, **9**, 312; B. L. Barnett, C. Krüger, Y.-H. Tsay, R. H. Summerville and R. Hoffmann, *Chem. Ber.*, 1977, **110**, 3900.
12 R. K. Brown, J. M. Williams, M. F. Fredrich, V. W. Day, A. J. Sivak and E. L. Muetterties, *Proc. Natl. Acad. Sci. USA*, 1979, **76**, 2099; R. G. Teller, J. M. Williams, T. F. Koetzle, R. R. Burch, R. M. Gavin and E. L. Muetterties, *Inorg. Chem.*, 1981, **20**, 1806; M. D. Fryzuk, W. E. Piers, F. W. B. Einstein and T. Jones. *Can. J. Chem.*, 1989, **67**, 883.
13 E. B. Meier, R. R. Burch, E. L. Muetterties and V. W. Day, *J. Am. Chem. Soc.*, 1982, **104**, 2661; D. L. Thorn and J. A. Ibers, *Adv. Chem. Ser.*, 1982, **196**, 117.
14 G. V. Goeden, J. C. Huffman and K. G. Caulton, *Inorg. Chem.*, 1986, **25**, 2484.
15 (*a*) L. Mole, J. L. Spencer, N. Carr and A. G. Orpen, *Organometallics*, 1991, **10**, 49; (*b*) N. Carr, L. Mole, A. G. Orpen and J. L. Spencer, *J. Chem. Soc., Dalton Trans.*, 1991, 863; (*c*) L. Mole, J. L. Spencer, N. Carr and A. G. Orpen, *J. Chem. Soc., Dalton Trans.*, 1992, 2653.
16 T. Yoshida, T. Yamagata, T. H. Tulip, J. A. Ibers and S. Otsuka, *J. Am. Chem. Soc.*, 1978, **100**, 2063.
17 S. A. Litster, L. Mole, A. D. Redhouse and J. L. Spencer, *Acta Crystallogr., Sect. C*, 1992, **48**, 913.
18 A. Dedieu and R. Hoffmann, *J. Am. Chem. Soc.*, 1978, **100**, 2074.
19 C. J. Moulton and B. L. Shaw, *J. Chem. Soc., Chem. Commun.*, 1976, 365.
20 Siemens SHELXTL, G. M. Sheldrick, SHELXTL PLUS, University of Göttingen, 1989.

Received 8*th December* 1995; *Paper* 5/08006A